0026-895X/06/6906-1913–1923$20.00
MOLECULAR PHARMACOLOGY
Copyright © 2006 The American Society for Pharmacology and Experimental Therapeutics
Mol Pharmacol 69:1913–1923, 2006

Vol. 69, No. 6
20792/3111459
Printed in U.S.A.

Transactivation of Rat Apical Sodium-Dependent Bile Acid Transporter and Increased Bile Acid Transport by 1α,25-Dihydroxyvitamin D_3 via the Vitamin D Receptor

Xianghai Chen, Frank Chen, Shanjun Liu, Hartmut Glaeser, Paul A. Dawson, Alan F. Hofmann, Richard B. Kim, Benjamin L. Shneider, and K. Sandy Pang

Departments of Pharmacology (X.C., K.S.P.) and Pharmaceutical Science (S.L., K.S.P.), University of Toronto, Toronto, Ontario, Canada; Division of Pediatric Hepatology, Department of Pediatrics, Mount Sinai School of Medicine, New York, New York (F.C., B.L.S.); Division of Clinical Pharmacology, School of Medicine, Vanderbilt University, Nashville, Tennessee (H.G., R.B.K.); Department of Internal Medicine, Wake Forest University School of Medicine, Winston-Salem, North Carolina (P.A.D.), and Division of Gastroenterology, School of Medicine, University of California at San Diego, La Jolla, California (A.F.H.)

Received November 12, 2005; accepted February 15, 2006

ABSTRACT

Transactivation of the rat apical sodium-dependent bile acid transporter (ASBT; Slc10a2) by 1α,25-dihydroxyvitamin D_3 [1,25$(OH)_2D_3$] via the vitamin D receptor (VDR), was studied. Levels of ASBT protein and mRNA were low in the duodenum and high in the ileum, and both were induced by 1,25$(OH)_2D_3$. The nuclear receptor protein, VDR, was present uniformly in the duodenum, jejunum, and ileum of the rat small intestine. The physiological relevance of ASBT induction by 1,25$(OH)_2D_3$ was assessed by measuring absorption of cholylsarcosine, a non-metabolized synthetic bile acid analog, from duodenal or ileal closed loops of the perfused rat small intestine preparation. Absorption of cholylsarcosine was much greater from the ileal segment (28-fold that of the duodenum under control conditions) and was enhanced with 1,25$(OH)_2D_3$ treatment. Transient transfection analysis of the rat ASBT promoter in Caco-2 cells revealed concentration-dependent enhancement of luciferase reporter activity after treatment with 1,25$(OH)_2D_3$. The activation by 1,25$(OH)_2D_3$ was abrogated after site-directed mutagenesis or deletion of the vitamin D response element (VDRE) in the ASBT promoter. Gel-shift mobility assays of nuclear extracts from rat ileum showed that both rat retinoid X receptor and VDR were bound to the VDRE. The results indicate that rat ASBT gene expression is activated by 1,25$(OH)_2D_3$ by specific binding to the VDRE and that such activation enhances ileal bile acid transport. Human ABST mRNA and promoter activity were also increased in Caco-2 cells treated with 1,25$(OH)_2D_3$, suggesting a physiological role of VDR in human ileal bile acid homeostasis.

The enterohepatic circulation of bile acids (BAs) is critical for the maintenance of BA homeostasis. In the liver, BA synthesis from cholesterol is under feedback regulation that operates through orphan nuclear receptors (Goodwin et al., 1999). BAs are natural ligands of the farnesoid nuclear receptor (FXR), which transcriptionally activates the short heterodimer partner (SHP). SHP in turn can decrease hepatic bile acid synthesis by antagonizing the liver receptor homolog 1 (LRH-1), a competence factor required for expression of the CYP7A1 gene in the liver (Goodwin et al., 1999). FXR also up-regulates the bile salt export pump (Ananthanarayanan et al., 2001), whereas it down-regulates the sodium-dependent taurocholate cotransporting polypeptide in the liver (Denson et al., 2001). In the intestine, changes in absorption of BAs alter the BA pool size and affect cholesterol metabolism (Lewis et al., 1995; Xu et al., 2000). The apical sodium-dependent bile acid transporter (ASBT; SLC10A2) is largely responsible for BA absorption and is abundantly expressed in the distal ileum (Shneider et al., 1995). Efflux occurs via the recently cloned organic solute transporters α

This work was supported by Canadian Institutes of Health Research grant MOP64350 (to K.S.P.) and National Institutes of Health grants DK47987 (to P.A.D.), GM31304 and GM54724 (to R.B.K.), and DK54165 (to B.L.S.).

X.C. and F.C. contributed equally to this work.

Article, publication date, and citation information can be found at http://molpharm.aspetjournals.org.
doi:10.1124/mol.105.020792.

ABBREVIATIONS: BA, bile acid; FXR, farnesoid X nuclear receptor; SHP, short heterodimer partner; LRH-1, liver receptor homolog 1; ASBT apical sodium-dependent bile acid transporter; MRP, multidrug resistance associated protein; ILBP, ileal lipid binding protein; VDR, vitamin D receptor; RXR, retinoid X receptor; 1,25$(OH)_2D_3$, 1α,25-dihydroxyvitamin D_3; CS, cholylsarcosine; VDRE, vitamin D response element; [^{3}H]CS, 22,23-[^{3}H]cholylsarcosine; HPLC, high-performance liquid chromatography; S, segment; PMSF, phenylmethylsulfonyl fluoride; DTT, dithiothreitol; PBS, phosphate-buffered saline; RT-PCT, reverse transcription-polymerase chain reaction; PCR, polymerase chain reaction; kb, kilobase(s); SSC, standard saline citrate; TK, thymidine kinase; SV, simian virus; DMSO, dimethyl sulfoxide.

and β (Dawson et al., 2005) and the multidrug resistance-associated protein (MRP) 3 (McCarthy et al., 2005), unrelated transporters that are implicated in basolateral efflux of the BAs.

It is, therefore, not surprising that ASBT expression is highly regulated. The molecular mechanisms responsible for the regulation of ASBT, particularly those involving the FXR-dependent pathway, are beginning to be understood (Chen et al., 2003). In mice and rabbits, bile acids repress ASBT gene expression by acting through FXR to induce expression of SHP, which in turn antagonizes LRH-1, a competence factor required for ASBT expression (Chen et al., 2003). By contrast, the rat ASBT gene lacks the LRH-1 *cis*-acting element. Hence, there is a lack of BA-mediated repression of the rat ASBT (Chen et al., 2003). Rat ASBT gene expression is decreased by inflammatory cytokines (Chen et al., 2002), whereas the human ASBT gene is regulated by hepatocyte nuclear factor-1α, peroxisome proliferator-activated receptor α, retinoic acid receptor, and by vitamin A (Chen et al., 2002; Jung et al., 2002; Neimark et al., 2004). In both rat and human, dexamethasone and budesonide exert a major inducing effect on ASBT through the glucocorticoid nuclear receptor that is highly expressed in the ileum and colon (Jung et al., 2004). BAs also act through FXR to stimulate expression of the ileal bile acid binding protein (ILBP) that is postulated to offer cytoprotection against high intracellular concentrations of BAs (Kramer et al., 1998). BAs can further alter gene expression by non–FXR-dependent mechanisms. For example, lithocholic acid induces CYP3A4 in the colon via the vitamin D receptor (VDR) (Makishima et al., 2002), a classic nuclear receptor that exhibits significant homology with other members of the nuclear receptor superfamily: pregnane X receptor, constitutive androstane receptor, liver X receptor, FXR, and retinoid X receptor (RXR) (Mangelsdorf et al., 1995).

Although there is no direct evidence to suggest that vitamin D_3 or its active metabolite 1,25-dihydroxyvitamin D_3 [1,25$(OH)_2D_3$] regulates intestinal BA absorption, MRP3 mRNA is up-regulated by 1,25$(OH)_2D_3$ in the colon (McCarthy et al., 2005). In this study, we examined the role of VDR in rat ASBT expression and BA absorption and showed transactivation with 1,25$(OH)_2D_3$. We investigated the functional implication of the VDR transactivation of rat ASBT using a recirculating perfused rat small intestinal preparation and cholylsarcosine (CS), a nontoxic and well absorbed synthetic bile acid that does not undergo appreciable deconjugation and dehydroxylation (Schmassmann et al., 1990). The absorption of CS from the lumen of closed, 4-cm duodenal and ileal segments was compared. We then used deletion and site-directed mutagenesis to identify a functional vitamin D responsive element (VDRE) in the rat ASBT gene promoter and confirmed that the putative VDRE is functional in binding both the VDR and RXR proteins with gel-shift mobility assays.

Materials and Methods

Materials. 1,25$(OH)_2D_3$, as a 0.1% solution in ethanol, was obtained from BIOMOL Research Laboratories (Plymouth Meeting, PA). Unlabeled CS was a gift of the Diamalt Company (Raubling, Germany). [^{3}H]CS (22,23-[^{3}H]cholylsarcosine; specific activity 14 Ci/mmol) was synthesized as described by Sorscher et al. (1992) and purified to 98% radiochemical purity by high-pressure liquid chromatography. Bovine serum albumin in Tyrode's solution was purchased from Sigma-Aldrich Canada (Mississauga, ON, Canada), dextrose (50% injection USP) was obtained from Abbott Laboratories (Montreal, QC, Canada), and methanol (HPLC grade) was purchased from Fisher Scientific (Mississauga, ON, Canada). Other materials were obtained from Sigma-Aldrich Canada.

In Vivo Induction with 1,25$(OH)_2D_3$. Male Sprague-Dawley rats (295–310 g), bred by Charles River (St. Constant, QC, Canada) were given water and food ad libitum and maintained under a 12:12-h light and dark cycle in accordance to animal protocols approved by the University of Toronto (Toronto, ON, Canada). Induction was initiated by intraperitoneal injection of 0.27 μg/kg/day or 0.64 nmol/kg/day 1,25$(OH)_2D_3$ in 1.3 ml/kg corn oil and 0.02% ethanol for 4 days (Thierry-Palmer et al., 2002). Control animals received corn oil and 0.02% ethanol vehicle only.

Enterocyte Preparation. At the end of 4 days of 1,25$(OH)_2D_3$ treatment, the small intestine was removed on ice and divided into eight segments (Cong et al., 2001). Segment 1 (S1) encompasses the duodenum from the pyloric ring to the ligament of Treitz; segment 2 (S2) is a jejunal segment of equal length immediately distal to the ligament of Treitz. The remaining small intestine was then divided into six segments of equal length (S3 to S8, with S8 representing the ileum just proximal to the ileocecal valve). Enterocytes, harvested according to Traber et al. (1991) with modifications (Cong et al., 2001), were snap-frozen in liquid nitrogen and stored at −80°C. After thawing on ice, the enterocytes were mixed with equal volumes of lysis buffer (4 mM PMSF, 2 mM EDTA, 4 mM EGTA, 0.25 mM DTT, and 0.2 mM Na_2CO_3) and protease inhibitor cocktail, and sonicated for 10 s using a cell disruptor. After centrifugation of the cell lysate at 3000*g* (10 min), the supernatant was removed and centrifuged at 21,000*g* for 90 min at 4°C to yield a crude membrane preparation (Cong et al., 2001) and used for analyses of ASBT. Protein was assayed by the method of Lowry et al. (1951).

Western Blot Analysis. Enterocyte membrane proteins (15 μg) were separated on 7.5% or 10% SDS-polyacrylamide gels overlaid with a 4% acrylamide stacking gel; a standard S8 sample was included on each gel as a load control. The proteins were transferred to nitrocellulose membranes (GE Healthcare, Little Chalfont, Buckinghamshire, UK), followed by blocking of the nitrocellulose blots overnight at 4°C with 5% (w/v) nonfat dry milk in Tris-buffered saline containing 0.1% Tween 20. Anti-human ASBT antibody (1:700 dilution) (Shneider et al., 1995) was incubated overnight at 4°C, followed by washes in PBS containing 0.1% Tween 20, and then incubated with the secondary antibody, a peroxidase-conjugated goat anti-rabbit IgG (1:2000; Bio-Rad Laboratories, Mississauga, ON, Canada) for 1 h at room temperature. Nuclear protein extracts were prepared to measure the expression of VDR protein. In brief, 50 to 80 mg of harvested enterocytes were resuspended in 1 ml of homogenization buffer (0.25 M sucrose, 20 mM HEPES, pH 7.9, 10 mM KCl, 1.5 mM $MgCl_2$, 0.5 mM DTT, 0.5 mM spermidine, and 0.15 mM spermine), sonicated for 30 s at room temperature and then centrifuged for 10 min at 5000 rpm (approximately 2300*g*). The nuclei protein pellets were washed twice in 1 ml of PBS, resuspended in 300 to 400 μl of sample buffer (20 mM HEPES, pH 7.9, 25% glycerol, 0.42 M NaCl, 1.5 mM $MgCl_2$, 0.2 mM EDTA, 0.5 mM DTT, and 0.5 mM PMSF; 125 μl/10 ml of buffer), and the nuclei were disrupted using 15 to 20 passages through a 23-gauge needle. Samples containing 20 μg of enterocyte crude nuclear proteins were resolved on 10% SDS-polyacrylamide gels overlaid with 4% acrylamide stacking gel. The proteins were transferred to nitrocellulose membranes (GE Healthcare), followed by blocking of the nitrocellulose blots overnight at 4°C with 5% (w/v) nonfat dry milk in PBS containing 0.1% Tween 20. Rat anti-VDR antibody (1:1000 dilution; Research Diagnostics Inc., Flanders, NJ) was incubated overnight at 4°C, followed by washes in PBS containing 0.1% Tween 20, and then incubated with the secondary antibody, peroxidase-conjugated goat anti-rat IgG (1:5000; Santa Cruz Biotechnology, Santa Cruz, CA), for 1 h at room temper-

ature. The membranes were then stripped and incubated overnight at 4°C with anti-β-actin antibody (1:1000; Sigma-Aldrich Canada), washed, and incubated with the secondary antibody, peroxidase-conjugated goat anti-mouse IgG (1:5000; Vector Laboratories, Burlingame, CA), for 1 h at room temperature. Immunoreactive bands were visualized by chemiluminescence and quantified by scanning densitometry (NIH Image software; http://rsb.info.nih.gov/nih-image/). The intensity of the sample was normalized against that of β-actin to correct for protein loading and further normalized to a standard sample (S8 membrane preparation from one rat) that was present on all blots.

Reverse Transcription-Polymerase Chain Reaction and Real-Time Polymerase Chain Reaction. Total RNA was obtained from 30 to 100 mg of intestinal tissue using the TRIzol extraction method (Invitrogen, Carlsbad, CA) (Chomczynski and Sacchi, 1987) or the RNeasy mini kit (QIAGEN, Mississauga, ON, Canada). For the TRIzol-extracted samples, a DNA digest was performed to remove any genomic DNA using the Turbo-DNA-free kit (Ambion, Austin, TX) according to the manufacturer's instructions. RT-PCR was performed using the QIAGEN OneStep RT-PCR kit and the primers shown in Table 1. For ASBT, 2 μg of template RNA was used for each reaction, whereas 1 μg of template was used to detect β-actin. The reverse transcription for ASBT was carried out at 50°C for 30 min. The PCR conditions for rat ASBT used 30 cycles of a denaturing step at 94°C for 1 min, annealing at 60°C for 1 min, and extension at 72°C for 1 min. All expression data were standardized to β-actin that was determined in the same analysis.

Real-Time PCR was also performed using the iCycler iQ real-time detection system (Bio-Rad, Hercules, CA). The cDNA synthesis was performed with 1 μg of total RNA using the TaqMan reverse transcription reagents kit (Applied Biosystems, Foster City, CA) according to the manufacturer's instructions. In brief, PCRs were carried out in a 50-μl reaction using 5 μl of cDNA template. The primers used for ASBT and 18S are shown in Table 1 (Hulzebos et al., 2003; Su and Waxman, 2004). The PCR reactions were performed using the Bio-Rad iQ SYBR Green Supermix. PCR was initiated with a denaturation step at 95°C for 3 min, followed by 40 cycles of 95°C for 15 s (denaturation step) and 60°C for 30 s (extension step) for ASBT, and 34 cycles of 95°C for 15 s (denaturation step) and 65°C for 60 s (extension step) for the 18S-RNA. A calibration curve using purified PCR products was performed to calculate the copy number of the samples using the iCycler iQ Optical system software version 3.0a (Bio-Rad). The calculated copy number of ASBT was normalized to the copy number of the 18S RNA.

Northern Blot Analysis. For the Northern blot analysis, 10 μg of total RNA from the rat enterocytes as well as Caco-2 cells was resolved on a 1% agarose gel containing 1.6 M formaldehyde electrophoresis, transferred to nylon membranes (Osmonics Inc., Westborough, MA) by capillary action, and UV cross-linked using a Stratalinker (Stratagene, La Jolla, CA). [^{32}P]dCTP (3000 Ci/mmol; 10 mCi/ml), obtained from Invitrogen, was used for random primed labeling of the cDNA probes. The 1.2-kb insert of the rat ileal ASBT clone BS37C1 (Shneider et al., 1995) that was excised by digestion with EcoRI and XhoI, full-length ILBP (mouse ILBP cDNA probe from Dr. Jeffrey Gordon, Washington University, St. Louis, MO) (Crossman et al., 1994), and mouse SHP and FXR (Neimark et al., 2004) were used as templates to generate the ^{32}P-labeled probes. Blots were sequentially hybridized with radiolabeled rat and human ASBT, ILBP, FXR, and SHP cDNA probes (Chen et al., 2001; Neimark et al., 2004). The blots were washed twice with 6× SSC for 5 min at room temperature, with 2× SSC for 30 min at 60°C, and twice with 0.1× SSC for 30 min at room temperature. Signal intensity was determined using a PhosphorImager (GE Healthcare). The same blots were reprobed with a 28S RNA oligonucleotide probe to correct for differences in RNA sample loading.

Cell Culture. The human colon epithelial Caco-2 cells (HTB-37; American Type Culture Collection, Manassas, VA) were used for transfection. Cells were grown at 37°C and in a 5% CO_2 atmosphere in Dulbecco's modified Eagle's medium supplemented with 4 mM L-glutamine, 1.5 g/l $NaHCO_3$, 4.5 g/l glucose, 1 mM sodium pyruvate, 0.1 mg/ml human transferrin, and 10% fetal calf serum. The rat ASBT promoter constructs containing the putative VDRE (Table 2) were transfected into Caco-2 cells and treated with various concentrations of 1,25$(OH)_2D_3$ (0–100 nM) for 40 h. Cells were then harvested to determine the ASBT promoter-directed luciferase expression. A thymidine kinase (TK)-promoter driven *Renilla reniformis* luciferase containing the SV40 promoter was cotransfected in these experiments and used as a control for transfection efficiency. All transfections were performed in triplicate and repeated in three sets of experiments.

Rat ASBT Plasmid Constructs. Two plasmid constructs containing the rat ASBT promoter sequences (Chen et al., 2001) were used in the present studies. The pGL3-ASBT5′/$^{-2685/+384}$ construct encompassed the 3.1 kb of rat ASBT 5′ promoter sequence that

TABLE 1
Oligonucleotides used for real-time PCR and RT-PCR

Oligonucleotide	Forward Sequence (5′ to 3′)	Reverse Sequence (5′ to 3′)
RT-PCR		
ASBT primer (exon 2)	ACCACTTGCTCCACACTGCTT	CGTTCCTGAGTCAACCCACAT
β-Actin	AGCCATGTACGTAGCCATCCA	TCTCCGGAGTCCATCACAATG
Real-time PCR		
ASBT primer	AGGCTGTGGTGGTGCTAATTATG	CAGAGAAATGCCTGAGGTCCAT
18 S primer	GTAACCCGTTGAACCCCATT	CCATCCAATCGGTAGTAGCG

TABLE 2
Comparison of VDRE-like motifs in rat ASBT promoter to published VDREs
Nucleotides identical to the VDRE consensus sequence are underlined. Consensus VDRE was determined by binding of VDR/RXR heterodimers to randomly selected high-affinity VDRE.

Source	Sequence	Identity	Position (5′ to 3′)	Reference
		%		
Consensus VDRE	PuGGTCANNGPuGTTCA	100		Zierold et al. (1994)
Rat ASBT direct repeat 3	AGAAGTGGGAGGAGA	60	−2131/−2117	Chen et al. (2001) (GenBank accession no. AF285154)
Rat 24-OHase-distal	GGTTCAGCGGGTGCG	80	−259/−245	Zierold et al. (1995)
Human osteocalcin	GACTCACCGGGTGAA	73		Ozono et al. (1990)

Pu, A or G.

contained a potential VDRE-like *cis*-element (5′-AGAAGTGGGAGGAGA-3′) between positions −2131 and −2117 (Table 2). The second promoter construct (pGL3-ASBT5′/$^{-829/+384}$) is transcriptionally active, but it lacks any potential VDRE-like *cis*-elements (Chen et al., 2001).

Human ASBT Plasmid Construct. A hybrid plasmid construct containing 0.6-kb (−337 to +297) of the human ASBT promoter (Neimark et al., 2004) was used. The construct includes a VDRE-like direct repeat 3 AGGGAAATGGGAGAA (−325/−311) that is similar to the sequence GACTCACCGGGTGAA of the human osteocalcin gene (Kerner et al., 1989; Ozono et al., 1990) (Table 2).

Site-Directed Point Mutagenesis of VDRE *cis*-Element. Site-directed mutagenesis was performed to investigate the role of the VDRE-mediated *cis-trans* interactions in the regulation of the rat ASBT 5′ promoter. A pair of oligonucleotides containing two point mutations in the VDRE sequence were synthesized as primers (Oligonucleotide Core Facility, Mount Sinai School of Medicine, New York, NY) and a QuikChange site-directed mutagenesis kit (Stratagene) was used to introduce the specific mutations into pGL3-ASBT5′/$^{-2685/+384}$. The VDRE-like element was targeted by primers ranging from −2139 to −2109 as shown by the sequence 5′-GCAGAGCC-AGAc(**A**)GTGGGAGt(**G**)AGAGACCTTG C-3′. The VDRE sequence (underlined) is from −2131 (5′) to −2117 (3′); *c* (−2128) and *t* (−2120) are the point mutation sites, and the **A** and **G** within parentheses are the original nucleotides. After site-directed mutagenesis, the resultant mutant plasmid construct, pGL3-ASBT5′/VDRE^{mu}, was examined by electrophoresis, and the point mutations were confirmed by DNA sequencing.

Luciferase Reporter Assays. Transient transfection of Caco-2 cells and luciferase activity measurements were carried out as described previously (Chen et al., 2001). In brief, 5×10^6 cells were transfected by electroporation with 4 μg of the indicated rat and human plasmid constructs, plus 0.1 μg of a quantitative control plasmid pRL-TK (Promega, Madison, WI) containing a TK promoter-driven *R. reniformis* luciferase gene. Then, the cells were cultured for an additional 40 h with $1,25(OH)_2D_3$, and harvested to determine the luciferase activity using the standard procedures. As a control for specificity, the SV40 promoter-driven pGL3-luciferase construct (Promega) was transfected into Caco-2 cells and incubated with DMSO or $1,25(OH)_2D_3$. All transfections were performed in triplicate and repeated in three experiments.

Electrophoretic Mobility Shift Assays of Nuclear Protein Extracts from Rat Enterocytes. Nuclear extracts were prepared from vehicle control (corn oil or DMSO) or $1,25(OH)_2D_3$-treated S8 enterocytes or Caco-2 cells as described previously (Chen et al., 1997). In brief, 1×10^8 harvested enterocytes or Caco-2 cells were resuspended in 1 ml of buffer A (0.25 M sucrose, 20 mM HEPES, pH 7.9, 10 mM KCl, 1.5 mM $MgCl_2$, 0.5 mM DTT, 0.5 mM spermidine, and 0.15 mM spermine) and incubated for 5 min at room temperature. Then, 40 μl of lysolecithin (10 mg/ml) was added, and the cells were gently swirled for 90 s before addition of 2 volumes of ice-cold buffer B (3% bovine serum albumin in buffer A). Nuclei, pelleted by centrifugation at 1000*g* for 30 s, were washed twice in 2 ml of buffer B. After removal of the supernatant, 2 ml of buffer C (20 mM HEPES, pH 7.9, 25% glycerol, 0.42 M NaCl, 1.5 mM $MgCl_2$, 0.2 mM EDTA, 0.5 mM DTT, and 0.5 mM PMSF) was added per 10^8 cells. The nuclei were disrupted using 15 to 20 passages through a 23-gauge needle. After gentle stirring on ice, the mixture was centrifuged at 25,000*g* for 30 min, and the supernatant was removed and dialyzed overnight against buffer D (20 mM HEPES, pH 7.9, 20% glycerol, 0.1 M KCl, 0.2 mM EDTA, 0.5 mM DTT, and 0.5 mM PMSF). After further centrifugation at 25,000*g* for 20 min, the supernatant was divided into aliquots, quick-frozen, and stored at −80°C.

Band Shift Assays. Nuclear proteins (5 μg) were incubated at 37°C for 30 min with 2×10^5 dpm of ^{32}P-labeled DNA probe (25 pM) in 15 mM KCl, 5 mM $MgCl_2$, 0.25 mM EDTA, 0.25 mM DTT, 12 mM HEPES, pH 7.9, 10% glycerol, and *Escherichia coli* tRNA (200 ng/μl); the mixture was then digested with 1 μl of DNase I (127 units/μl; Life Technologies) for 30 min to remove the unbound DNA probes (Chen et al., 2001). The reaction mixture was incubated with 0.2 μg of mouse anti-human VDR monoclonal antibody or mouse anti-rat RXR monoclonal antibody (Santa Cruz Biotechnology). Samples were resolved by electrophoresis on a 7% native polyacrylamide gel using 0.5× Tris borate-EDTA running buffer. The gels were vacuum-dried and exposed to Kodak BioMax MS film at −80°C.

We further examined the role of $1,25(OH)_2D_3$, the VDRE, and the mutated VDRE on binding, with three oligonucleotides used as competitors. The presence of the 50 nM $1,25(OH)_2D_3$ did not inhibit the protein-DNA binding. The sequence of the specific competitor was the same as that shown in Fig. 8A. Three Gs at the sequence positions 10, 17, and 19 were changed to Cs as the mutated specific competitor sequence; the purpose of changing these G nucleotides was because they are highly conserved in the VDRE of all of the species examined by other groups (Table 2). The sequence of the nonspecific scrambled competitor is 5′-GACCTTGCGGAAGTGGAGCCAGAGAGGACAG-3′ and contains the same numbers of A, T, C, and G as those of the specific competitor. We used 5 μg of S8 nuclear proteins that was preincubated with the various competitors [1 or 2 nM unlabeled VDRE, the mutated VDRE oligonucleotide, or the nonspecific (scrambled) VDRE sequence] for 30 min, followed by incubation with the 25 pM ^{32}P-labeled VDRE probe for an additional 30 min.

Small Intestine Perfusion. During the 4 days of vehicle or $1,25(OH)_2D_3$ treatment, the rats were allowed free access to food and water. On the last day, food was removed and the animals were given a 5% glucose solution as drinking water, and in situ intestine perfusion was conducted the next day. All the procedures were performed in accordance with approved protocols of the University of Toronto Animal Care Committee. Small intestinal vascular perfusion was performed according to Cong et al. (2001). The 4-cm duodenal closed loop was chosen at 2 cm from the pylorus, whereas for the ileal 4-cm loop, as immediately proximal to ileocecal valve; the intestinal tissue was tied securely with double ligatures for the creation of the loops. The small intestine was perfused in situ with recirculation of the 200-ml reservoir blood perfusate, entering via the superior mesenteric artery and exiting through the portal vein at a flow rate of 8 ml/min at 37°C. Perfusate consisted of bovine erythrocytes (20%), freshly obtained and washed (a kind gift of Ryding-Regency Meat Packers Ltd., Toronto, ON, Canada), 2% bovine serum albumin (Tyrode's solution; Sigma-Aldrich Canada), and 0.3% glucose in Krebs-Henseleit bicarbonate solution, buffered to pH 7.4 and oxygenated with 95% oxygen, 5% carbon dioxide (BOC Gases, Brampton, ON, Canada). A cannula was inserted into the end of the lumen of the noninjected small intestine to collect the luminal exudates.

After a 20-min equilibration period, between 4.5 and 4.8 μmol of CS (with [^{3}H]CS; $7.9 \pm 4.1 \times 10^6$ dpm) was injected into the lumen of the 4-cm closed loop of duodenum or ileum, and absorption was examined for 90 min. Samples of the reservoir perfusate (1 ml) were taken at 0, 2.5, 7.5, 12.5, 17.5, 22.5, 27.5, 35, 45, 55, 65, 75, and 90 min after initiation of perfusion. The total sampling volume was 13 ml and was less than 7% of the total volume (200 ml). At the end of experiment, the volume of perfusate remaining in the reservoir was measured and added to the volume of perfusate sampled for mass and volume conservation considerations. The intestinal segments (injected or noninjected) were emptied of their luminal contents, washed twice with 3 ml of ice-cold saline, and the contents were pooled. The intestine was isolated from the carcass, gently blotted and weighed, and kept at −20°C until analysis. The viability of the in situ vascularly perfused intestine preparation was estimated according to the perfusion pressure, hematocrit, and perfusate volume recovery (Cong et al., 2001). The hematocrit of the blood perfusate was determined before and after each experiment by a hematocrit centrifuge.

Analytical Procedures. Unlabeled and radiolabeled CS as well as metabolites were quantified using the HPLC method of Rossi et al. (1987). Blood and not plasma perfusate was used because CS was found to distribute into red blood cells. [^{3}H]CS metabolites were not found in perfusate and luminal samples, as verified by HPLC. [^{3}H]CS was quantified using a calibration curve. Standards of [^{3}H]CS of known radioactivity in 25 μl of methanol were added 400 μl of blank blood perfusate or blank luminal fluid and used to construct a calibration curve. Perfusate blood or luminal fluid sample (400 μl) was added 25 μl of methanol. Acetonitrile (1.2 ml) was added to both the standards and samples for precipitation of protein. After mixing and centrifugation, 1300 μl of the supernatant was transferred into a 20-ml glass scintillation vial. Then, 1.5 ml of H_2O and 16 ml of scintillation fluor (Ready Safe; Beckman Coulter Canada, Mississauga, ON, Canada) were added to attain a miscible and clear solution before counting (model 5801; Beckman Coulter Canada). The total dpm of the sample was determined from the calibration curve.

The Shimadzu HPLC system, used for verification of purity, metabolite detection, and determination of the specific activity, consisted of an SCL-10A system controller, LC-10AT pump, DGU-14A degasser, FCV-10AL low-pressure solenoid valve unit, and SIL-10A XL autoinjector. A mobile phase of methanol and 0.01 M KH_2PO_4 [75:25 (v/v)], pH 5.35, flow rate of 0.7 ml/min, and Altima C18 reverse-phase column (4.6 $\times$ 250 mm, particle size, 10 μm; Altech Associates, Deerfield, IL) and precolumn (2.2 $\times$ 0.34 cm i.d. packed in this laboratory with Waters Bondapak C18/Corasil 37–55 μm) were used. The effluent was monitored at 205 nm with a Shimadzu SPD-10A UV detector. Data acquisition and integration were performed with the Star-Chrom LITE HPLC data system software (D-Star Instruments, Manassas, VA). The eluted fractions were collected at 1-min intervals (FC 204 fraction collector; Gilson, Middleton, WI) for liquid scintillation counting. The radiolabeled peak for [^{3}H]CS comigrated with the authentic CS standard, after correction for the delay time due to connection between the HPLC and fraction collector; the retention time was approximately 16 to 17 min. No metabolite was found.

Statistical Analysis. Data analysis was carried out by the Student's *t* test or analysis of variance for the comparison of two means, followed by Fisher's protected least significant difference post hoc test for multiple determinations. $P < 0.05$ was considered statistically significant.

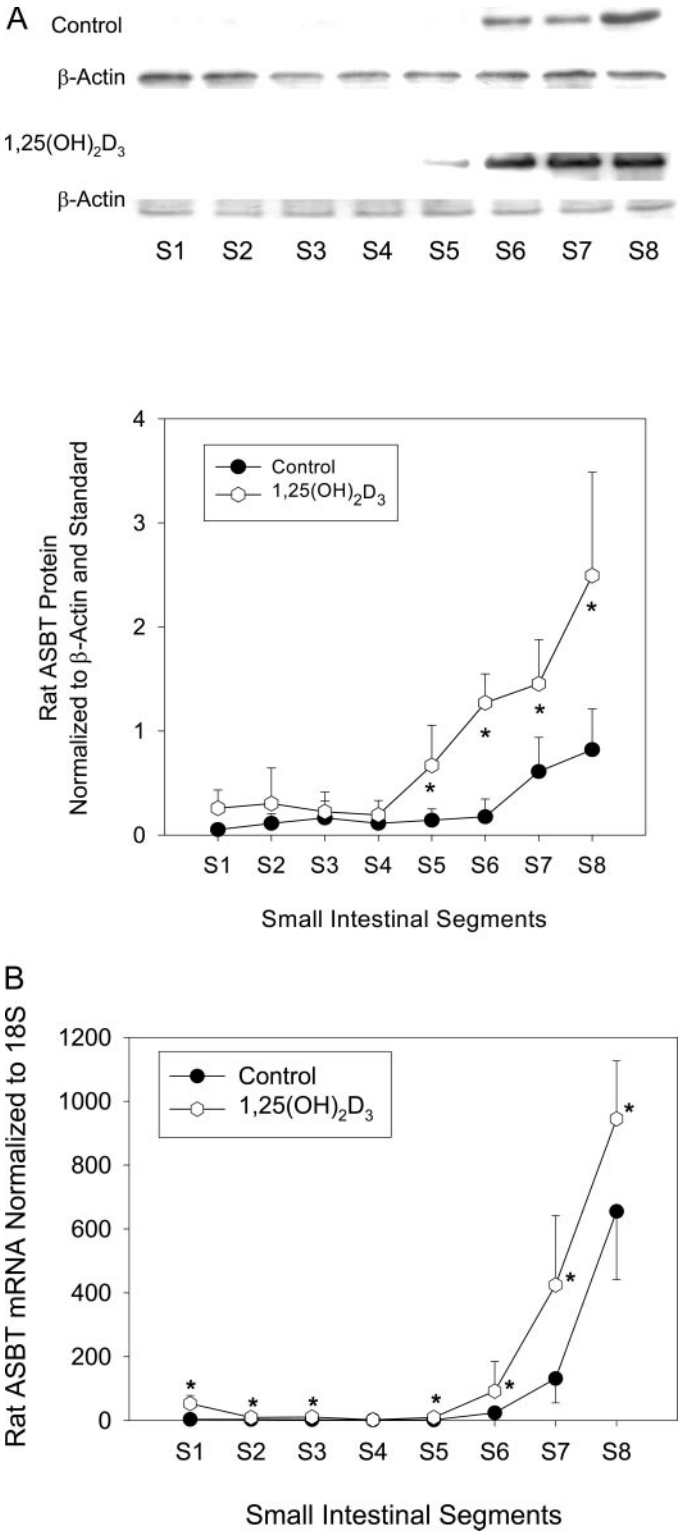

Fig. 1. Induction of rat ASBT protein and mRNA by $1,25(OH)_2D_3$ in rat enterocytes derived from small intestinal segments. Analysis of rat ASBT protein (A) and ASBT mRNA (B) in segmental enterocytes S1 (duodenum) to S8 (ileum) of rats treated with $1,25(OH)_2D_3$ (○) or vehicle (●) for 4 days. The data represent the mean ± S.D. of four preparations for protein and three to six samples for mRNA. *, $P < 0.05$ compared with control.

Results

Rat ASBT and VDR Proteins and ASBT mRNA in Enterocytes after 4-Day $1,25(OH)_2D_3$ Treatment. The expression of ASBT protein in the rat small intestine was

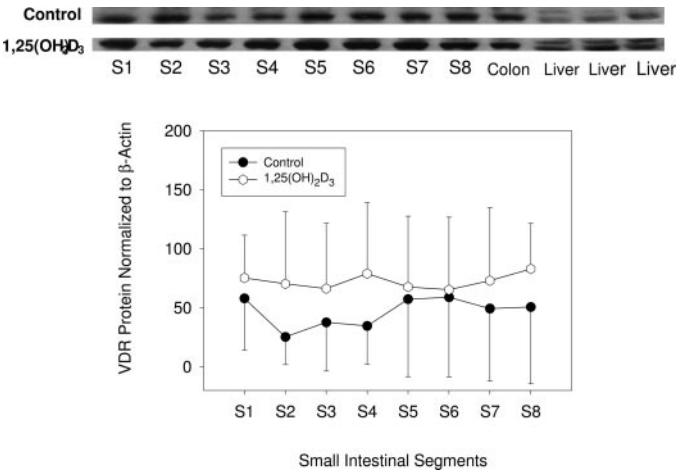

Fig. 2. Induction of rat VDR by $1,25(OH)_2D_3$ in rat enterocytes derived from small intestinal segments. Analysis of rat VDR protein in segmental enterocytes S1 to S8 of rats treated with $1,25(OH)_2D_3$ (○) or vehicle (●) for 4 days. The data represent the mean ± S.D. of three preparations. *, $P < 0.05$ compared with control.

predominantly distal, and only very low levels of ASBT protein expression were detected in the S1 to S5 preparations (Fig. 1A). Treatment with $1,25(OH)_2D_3$ increased the ASBT protein expression. Likewise, increased ASBT mRNA expression was detected using real-time PCR after $1,25(OH)_2D_3$ treatment (Fig. 1B); results from RT-PCR were similar (data not shown). The ASBT mRNA expression paralleled that of the protein and showed the greatest induction in the distal small intestine (S7 and S8) after $1,25(OH)_2D_3$ treatment (Fig. 1B). By contrast, the VDR protein was expressed at similar levels in all segments of the rat small intestine. Although the levels of VDR protein were slightly higher after $1,25(OH)_2D_3$ treatment, the changes were not significant (Fig. 2).

The inductive effect of $1,25(OH)_2D_3$ on ASBT mRNA expression in S8 was confirmed by Northern blot analysis. There was a significant (3-fold) increase in ASBT mRNA expression in rats treated with $1,25(OH)_2D_3$ (Fig. 3). The expression of ILBP and SHP mRNA was also increased after $1,25(OH)_2D_3$ treatment, although no change was observed for FXR mRNA. Expression of ASBT mRNA was low in the duodenum (S1) with real-time PCR analysis and was undetectable by Northern blot analysis in control and $1,25(OH)_2D_3$-treated rats (data not shown). Based on the negative results for ASBT, the expression of ILBP, FXR, and SHP mRNA was not examined in the rat duodenum.

Absorption of CS by the Vascularly Perfused Rat Small Intestine Preparation. CS occurred rapidly in the blood perfusate for both control and $1,25(OH)_2D_3$-treated small intestine preparations after absorption of the bolus dose (approximately 4.5 μmol) within the 4-cm closed loop. CS was not metabolized, as evident by the absence of metabolites in the perfusate and luminal fluid. The cumulative amount of CS absorbed from S8, the ileal segment, was significantly higher than that of S1, the duodenal segment (Fig. 4; Table 3). The extent of absorption of CS from the S8 loop at 90 min was almost complete for the $1,25(OH)_2D_3$-treated rats (85.2 ± 1.3% of dose) and was significantly higher than that of the control (66.2 ± 0.9% dose), with only a minor amount of CS being excreted into the noninjected intestinal lumen (2.7 ± 1.3 and 0.9 ± 0.2% dose). The amount of CS retained in the intestinal tissue was low and was less than 1% of the dose. The absorption of CS from the S1 loop was very low (2% dose at 90 min) and was only 1/28 that of S8 for the control small intestine preparation, showing that the contribution of S1 to CS absorption was very small (Fig. 4). With $1,25(OH)_2D_3$ treatment, CS absorption by S1 was significantly increased, albeit the absorption of CS was still very low compared with S8 (Table 3). All these observations were consistent with the changes in protein and mRNA levels of ASBT with $1,25(OH)_2D_3$ treatment (Fig. 1). The trend became apparent when the CS absorption rate [slope of the data up to 12.5 min of cumulative amount (percentage of dose was transformed as amounts) versus time; Fig. 4] was presented against rat ASBT protein and mRNA (Fig. 1). Only the early data points were considered such that the amount remaining in the lumen was not depleted. Positive correlations were found between the CS absorption rate in the perfused small intestine preparations and rat ASBT protein (Fig. 5A) as well as rat ASBT mRNA (Fig. 5B).

Identification of a Functional VDRE in the Distal Promoter of the Rat ASBT Gene: Induction of Rat ASBT Promoter Activity by $1,25(OH)_2D_3$. Examination of the rat ASBT promoter sequence revealed a potential VDRE (direct repeat motif, 5′-AGAAGTGGGAGGAGA-3′) located between positions −2131 and −2117 that was similar in sequence to the distal VDRE of the rat 25-hydroxyvitamin D_3 24-hydroxylase gene (Kerner et al., 1989; Ozono et al., 1990) (Table 2). To determine whether the VDRE-like sequence is responsible for the $1,25(OH)_2D_3$-induction of rat ASBT mRNA expression, Caco-2 cells were transfected with pGL3-ASBT5′/$^{-2685/+384}$ and treated with increasing concentrations of $1,25(OH)_2D_3$. As shown in Fig. 6, treatment with $1,25(OH)_2D_3$ increased the rat ASBT promoter activity in a concentration-dependent manner. Removal of the 5′ sequence from −2685 to −829 of pGL3-ASBT5′/$^{-2685/+384}$ abolished the activation by $1,25(OH)_2D_3$, further supporting a role of the putative VDRE at position −2131 to −2117 (Fig. 7A). Two point-mutations were also created in the 15-bp putative VDRE to test whether this sequence is responsible in mediating the induction by $1,25(OH)_2D_3$. As predicted, the mutant promoter construct, pGL3-ASBT5′/VDRE^{mu}, was ac-

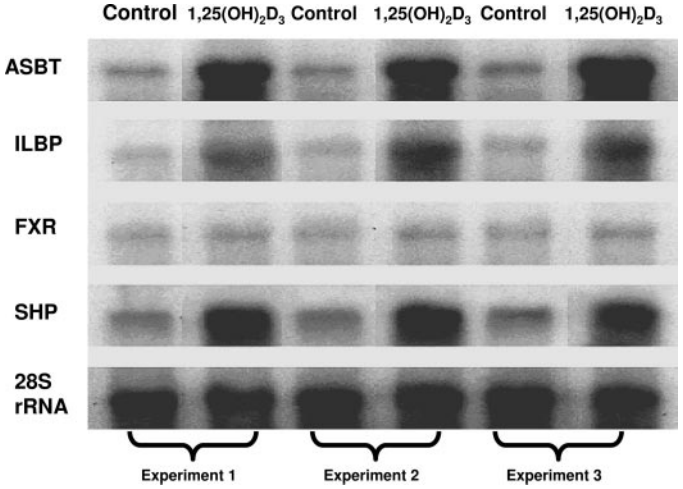

Fig. 3. Increased ileal expressions of rat ASBT, ILBP, and SHP mRNA by $1,25(OH)_2D_3$. Northern blot analyses were used to examine the mRNA levels of ASBT, ILBP, FXR, and SHP in 10 μg of total RNA isolated from S8 (ileal) enterocytes of rats treated with $1,25(OH)_2D_3$ or vehicle (control) for 4 days.

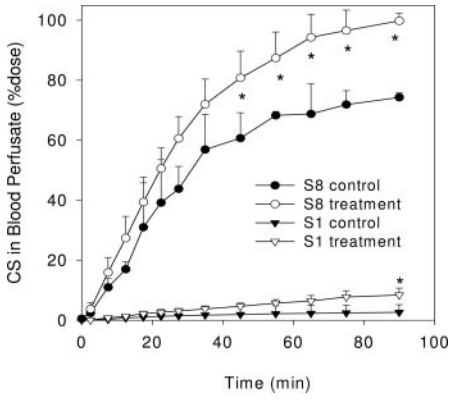

Fig. 4. Absorption of CS from 4-cm closed loop of duodenum (S1) or ileum (S8) in the recirculating vascularly perfused small intestine preparation, with or without treatment with $1,25(OH)_2D_3$ for 4 days. Vascular perfusion of the small intestine conducted on day 5 showed high absorption of CS from the ileum (S8) and the very low absorption from the duodenum (S1). *, $P < 0.05$, different from control.

tive but did not respond to $1,25(OH)_2D_3$ (Fig. 7B). The activity of VDRE-containing ASBT promoter was specific because the SV40 promoter-driven luciferase construct did not respond to DMSO or $1,25(OH)_2D_3$.

Confirmation of VDRE Properties by Band Shift Assay. Band shift assays were used to determine whether the VDR binds to the putative VDRE sequence identified in the rat ASBT promoter. DNA-protein complexes were observed after incubation of double-stranded rat ASBT-VDRE oligonucleotides with rat ileal enterocyte nuclear extracts (Fig. 8A, lane 2). The complex containing the ASBT VDRE was supershifted by antibodies directed against either the VDR (Fig. 8A, lane 3) or the RXR (Fig. 8A, lane 4). In contrast, antihistone antibodies did not alter migration of the rat ASBT-VDRE-protein complex (Fig. 8A, lane 5). Binding to the VDRE was specific, because dose-dependent competition was observed with unlabeled VDRE (sequence of Fig. 8A), but not for the mutated VDRE with the three G at the sequence positions 10, 17, and 19 substituted by C, nor for the nonspecific scrambled competitor of sequence 5′-GACCTTGCGGAAGTGGAGCCAGAGAGGACAG-3′ (Fig. 8B).

Responsiveness of Human ASBT to $1,25(OH)_2D_3$ and Similarities to Rat ASBT. To determine whether the human ASBT is also induced by $1,25(OH)_2D_3$, Northern blot analysis was used to examine the expression of human ASBT mRNA in Caco-2 cells after treatment with $1,25(OH)_2D_3$. As shown in Fig. 9A, expression of ASBT mRNA was significantly (273%) greater after $1,25(OH)_2D_3$ treatment. Endogenous levels of ILBP and SHP mRNA were significantly increased by 96 and 105%, respectively, in $1,25(OH)_2D_3$-treated Caco-2 cells, whereas no change was observed for FXR. These results suggest that the human ASBT promoter also harbors a VDRE (Table 2), and analysis of the proximal promoter region revealed a VDRE-like DR3 element (AGGGAAATGGGAGAA) located at position −325 to −311 (Table 2) (Kerner et al., 1989; Ozono et al., 1990). After transient transfection of a human ASBT promoter construct encompassing this region into Caco-2 cells and treatment with $1,25(OH)_2D_3$, the activity of the ASBT promoter construct was induced >4-fold (Fig. 9B). These results were similar to those observed for the rat ASBT promoter (Fig. 3).

Discussion

This is the first, comprehensive study that examines the transactivation of rat ASBT gene expression by $1,25(OH)_2D_3$. ASBT is the key transporter involved in the enterohepatic circulation of bile acids. Our results showed that rat ASBT protein and mRNA are virtually absent in the duodenum, but they are abundantly expressed in the distal small intestine under control conditions (Fig. 1). These observations are consistent with previous reports on the distal distribution of rat ASBT (Shneider et al., 1995). After $1,25(OH)_2D_3$ treatment, levels of expression of ASBT mRNA and protein were significantly increased, whereas their distribution patterns in small intestinal remained similar (Fig. 1, A and B). Consistent with these observations, absorption of CS from the closed loop at S1, the duodenal segment, of the vascularly perfused small intestine preparation was low, whereas CS absorption from the closed loop at S8, the ileal segment, was 28-fold that of S1 at 90 min (Fig. 4). Upon induction, the rate and extent of CS absorption by S8 was significantly greater, whereas the absorption of CS from S1 remained low, confirming that the duodenal contribution to BA absorption is negligible (Fig. 4; Table 3). The positive correlation between CS absorption with ASBT protein and mRNA further suggests that regulation of BA absorption by $1,25(OH)_2D_3$ occurred at the transcriptional level (Fig. 5). It was noteworthy that induction for mRNA of human ASBT in Caco-2 cells (Fig. 9A) and increased human ASBT promoter activity were observed with $1,25(OH)_2D_3$ treatment. The similar responses of the human ASBT to those of rat ASBT suggest a regulatory role of $1,25(OH)_2D_3$ on human ASBT.

Genes that respond to $1,25(OH)_2D_3$ typically contain a VDRE in their regulatory region to allow for activated VDR, a ligand-inducible, transcriptional, regulatory protein, to associate near the basal transcriptional machinery. Activated VDR first binds to RXR to form a stable protein-DNA heterodimeric complex, and then it binds to VDREs that consist of hexameric motifs in a direct repeat or inverted palindromic arrangement of the consensus sequence G(A)GT(G)TCA (Zierold et al., 1994). By computer analysis, we identified a potential VDRE-like element in the rat ASBT promoter that

TABLE 3

Summary of volumes and dose recoveries, and extents of absorption and excretion after intraluminal injection of labeled cholylsarcosine into 4-cm closed loops of the duodenum (S1) or ileum (S8) of the vascularly perfused rat small intestine, with and without 1α,25-dihydroxyvitamin D_3 treatment

Data are mean ± S.D.

	Duodenum Segment (S1)		Ileum Segment (S8)	
	Control	$1,25(OH)_2D_3$	Control	$1,25(OH)_2D_3$
No. of preparations	3	3	3	3
Dose (μmol)	4.8 ± 0.4	4.8 ± 0.6	4.5 ± 0.4	4.8 ± 0.4
Rat weight (g)	311 ± 22	300 ± 36	285 ± 14	316 ± 15
Injected intestine weight (g)	0.21 ± 0.03	0.19 ± 0.01	0.38 ± 0.03	0.33 ± 0.06
Whole intestine weight (g)	5.95 ± 0.29	5.92 ± 0.40	4.52 ± 0.12	5.59 ± 0.34[a]
Volume recovery (%)	85.0 ± 3.0	84.2 ± 1.0	86.7 ± 1.2	83.2 ± 2.1
Radioactivity at 90 min (%dose)				
Reservoir	2.3 ± 2.1	7.2 ± 2.0[a]	66.2 ± 0.9	85.2 ± 1.3[a]
Luminal fluid				
Injected lumen	61.9 ± 9.7	59.8 ± 13.2	9.1 ± 4.3	17.5 ± 9.0
Noninjected lumen	0.7 ± 0.9	0.6 ± 0.4	0.9 ± 0.2	2.7 ± 1.3
Intestine tissue				
Injected	10.5 ± 3.8	6.4 ± 0.5	0.7 ± 0.3	0.4 ± 0.7
Noninjected	1.0 ± 0.6	1.9 ± 1.1	0.7 ± 0.1	0.2 ± 0.4
Total dose recovery	76.3 ± 5.0	76.0 ± 12.2	77.5 ± 4.9	106 ± 11.8[a]

[a] $1,25(OH)_2D_3$ treatment was significantly different ($P < 0.05$) from control.

contained the direct repeat motif 5′-AGAAGTGGGAGGAGA-3′ (Table 2). The sequences showed limited similarity to the rat 25-hydroxyvitamin D_3 24-hydroxylase and human osteocalcin (5′-GACTCACCGGGTGAA-3′) VDREs (Table 2). The 25-hydroxyvitamin D_3 24-hydroxylase gene is the most responsive $1,25(OH)_2D_3$ target gene identified in mammals and has two VDREs located in the promoter region. A distal VDRE is located at position −259 and a proximal VDRE located at position −152 (Zierold et al., 1994, 1995). The proximity of the two sites to one another and to the transcription start site contributes to the strong responsiveness of the 24-hydroxylase gene to $1,25(OH)_2D_3$.

For determination of whether the potential VDRE in the rat ASBT promoter is functional (Fig. 7A, construct I), promoter constructs containing a point-mutated VDRE (Fig. 7B, construct III) or a VDRE sequence deletion (Fig. 7A, construct II) were generated. After transfection of the ASBT promoter constructs lacking the potential VDRE or containing a point-mutated VDRE into Caco-2 cells, marked differences in promoter activity were observed in response to $1,25(OH)_2D_3$ treatment, confirming that the proposed VDRE-like motif is functional (Fig. 7). Electrophoretic mobility shift assays using anti-VDR and anti-RXR antibodies for supershift analysis further confirmed that the VDR heterodimer binds specifically to the proposed VDRE in the rat ASBT gene promoter (Fig. 8). Hence, we conclude that $1,25(OH)_2D_3$ is able to directly activate rat ASBT gene expression at the transcriptional level through the binding of the hormone bound VDR/RXR heterodimer to rat ASBT-VDRE.

VDREs have been identified in a number of $1,25\text{-}(OH)_2D_3$ target genes, including osteocalcin (Kerner et al., 1989; Ozono et al., 1990), 25-hydroxyvitamin D_3 24-hydroxylase (Chen and DeLuca, 1995), calbindin-D_{28}k (Macdonald et al., 1992), and the glucocorticoid receptor (Morrison and Eisman, 1993). The administration of $1,25(OH)_2D_3$ is also known to induce VDR expression (Strom et al., 1989). In this study, slightly higher VDR protein levels were observed upon $1,25(OH)_2D_3$ treatment; however, the changes were too variable to show significance ($P > 0.05$) (Fig. 2). The VDR target genes include other transporters and enzymes, including the type II renal sodium-dependent inorganic phosphate transporter (Taketani et al., 1998), the sodium-sulfate cotransporter (Dawson and Markovich, 2002), the multidrug resistance-associated protein MRP3 (McCarthy et al., 2005), and the human CYP3A4 (Thummel et al., 2001). The hydroxysteroid sulfotransferase (SULT2A1) gene is also transactivated by VDR, in addition to pregnane X receptor and FXR (Echchgadda et al., 2004).

The present findings reveal a novel network of interactions that includes the VDR among nuclear receptors in controlling BA absorption. All of the small intestinal segments, the duodenum, jejunum and ileum, express similar levels of VDR (Fig. 2) and are apt to transactivate ASBT. The administration of $1,25(OH)_2D_3$ also led to increases in rat ILBP and SHP

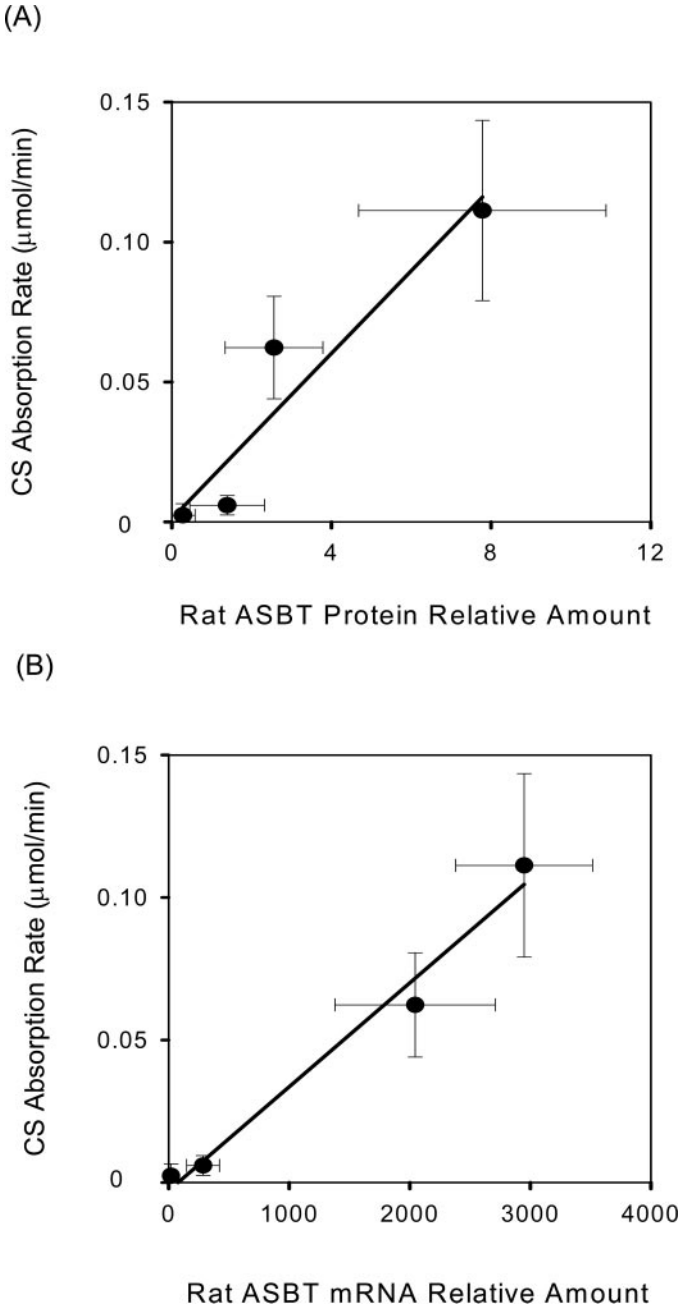

Fig. 5. Correlation between CS absorption and rat ASBT protein (A) and mRNA (B). Positive correlation was found between the cholylsarcosine absorption rate in the perfused rat small intestine preparation versus rat ASBT protein, expressed as relative intensity per microgram of protein (A), and rat ASBT mRNA, expressed as relative intensity per μg protein (B). The absorption rates were obtained as slopes of the cumulative amount (data from Fig. 4, percentage dose was transformed as micromoles) versus time plot for data up to 12.5 min; these rates correlated well against the relative amounts of rat ASBT protein and mRNA shown in Fig. 1.

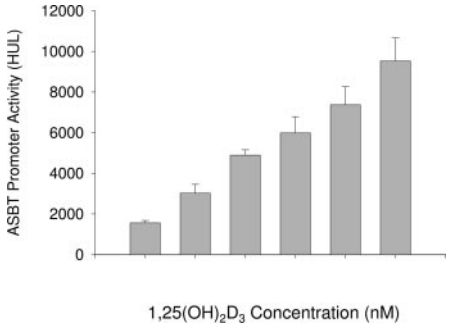

Fig. 6. Regulation of rat ASBT promoter expression by $1,25(OH)_2D_3$. Concentration-dependent $1,25(OH)_2D_3$ stimulation of rat ASBT promoter (pGL3-ASBT5′/$^{-2685/+385}$) activity in transfected Caco-2 cells in the luciferase reporter assay.

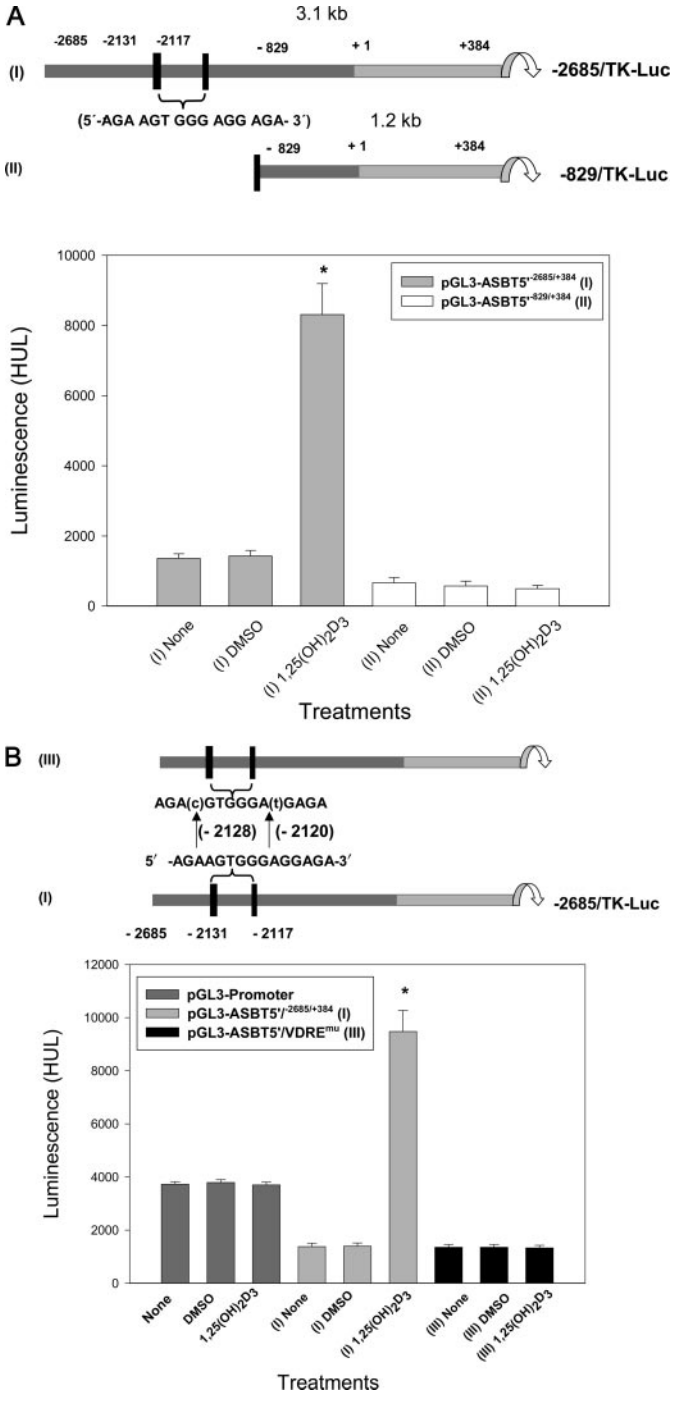

Fig. 7. The rat ASBT promoter and regulation by $1,25(OH)_2D_3$: the analysis of rat ASBT promoter truncations (A) or point-mutated VDRE sequences (B) in transfected Caco-2 cells. Plasmid constructs encompassing the promoter region containing an intact VDRE (construct I; pGL3-ASBT5′/$^{-2685/+385}$), a deletion of the putative VDRE (construct II; pGL3-ASBT5′/$^{-829/+384}$), or a point-mutated VDRE (construct III; pGL3-ASBT5′/VDRE^{mu}) upstream of a luciferase reporter were transfected into Caco-2 cells. The transfected cells were then treated with 100 nM $1,25(OH)_2D_3$ in DMSO for 40 h before harvest for the luciferase assays. To examine the nonspecific effect of $1,25(OH)_2D_3$ on the promoter activity, cells were transfected with a control plasmid construct, pGL3-promoter, that contained a SV40-driven luciferase gene (A) The basal activity of the shorter promoter construct (II) was reduced. Only the intact promoter encompassing the putative VDRE (15-bp motif, 5′-AGAAGTGGGAGGAGA-3′) showed increased activity with $1,25(OH)_2D_3$ pretreatment compared with those of controls (A). This activity disappeared upon site-directed mutagenesis (B). *, $P < 0.05$, different from the SV40 pGL3-promoter construct control.

mRNA levels, although FXR mRNA was unchanged (Fig. 3), a finding that is different from BA feeding to the ileum that typically leads to FXR-mediated activation of both SHP and ILBP but feedback inhibition of ASBT (Xu et al., 2000; Neimark et al., 2004). Thus, the bile acid-mediated responses of ILBP and ASBT are typically opposite. Upon administration of $1,25(OH)_2D_3$, there is a direct stimulation of ASBT, and the enhanced expression of ASBT is accompanied by increased flux of bile acids through the ileum. With $1,25(OH)_2D_3$ treatment, the expression of ILBP and SHP is elevated. We speculate that this increase is secondary to induction of ASBT expression leading to an increased flux of bile acids through the ileum and activation of FXR. However, a direct effect or other indirect effects of $1,25(OH)_2D_3$ cannot be excluded. Because the rat ASBT promoter lacks an LRH-1 binding site, the increased expression of SHP is not expected to reduce ASBT expression. However, the response of the human, mouse, or rabbit ASBT to $1,25(OH)_2D_3$ may be more

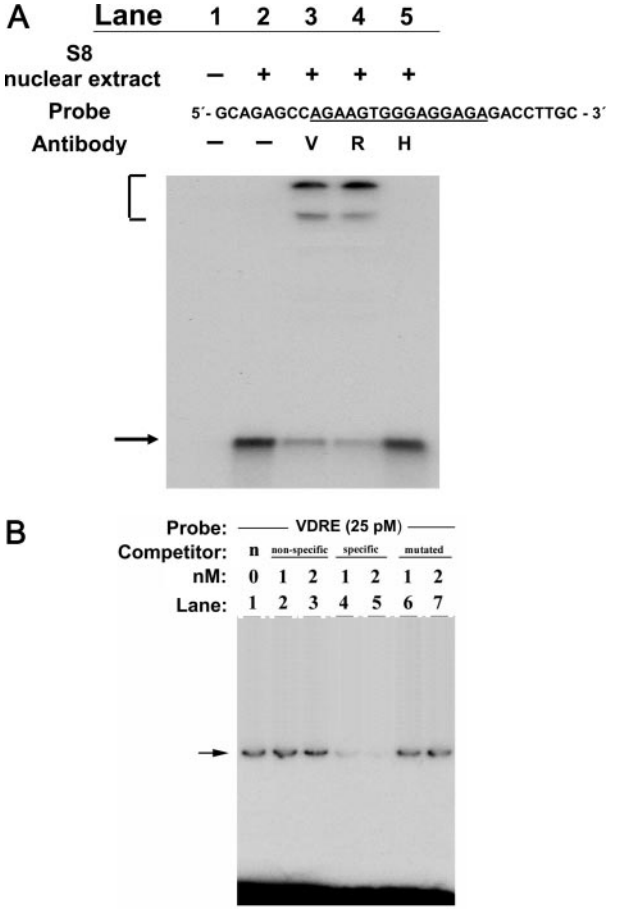

Fig. 8. The VDRE sequence identified in the rat ASBT promoter binds VDR and RXR (A) and competition of binding by 1 or 2 nM unlabeled VDRE and VDRE of mutated or scrambled sequence with 25 pM ^{32}P-labeled probe (B). Electrophoretic mobility shift assays using nuclear extracts isolated from rat ileal (S8) enterocytes. The addition of anti-VDR (V) and anti-RXR (R) and not anti-histone (H) antibodies resulted in binding, a supershift (bracket), and disappearance of the lower DNA-protein complex (arrow). The putative rat ASBT-VDRE in the oligonucleotide probe is underlined. B, competition for binding by unlabeled VDRE to rat S8 nuclear extracts was observed in lanes 4 and 5 compared with control (lane 1, "n" for no treatment). Neither nonspecific oligonucleotides (lanes 2 and 3) nor mutated VDRE oligonucleotides (lanes 6 and 7) were able to compete with wild-type VDRE for binding to rat S8 nuclear extracts. See text for details.

difficult to predict because the ASBT promoters in these species include a functional LRH-1 site.

In summary, this study shows that $1,25(OH)_2D_3$ directly transactivated the ASBT gene via the VDR, occurring through binding of VDR/RXR to the ASBT-VDRE site of the promoter. $1,25(OH)_2D_3$ increased both rat ASBT protein and ASBT mRNA, and the physiological importance of the transactivation was demonstrated by increased cholylsarcosine absorption in the small intestine. Although many nuclear receptors or coactivators (Goodwin et al., 1999; Ananthanarayanan et al., 2001; Jung et al., 2002, 2004; Makishima et al., 2002; Chen et al., 2003) have been implicated in BA homeostasis, none have been shown to up-regulate ASBT. Hence, VDR should be included as an important regulatory pathway in BA homeostasis.

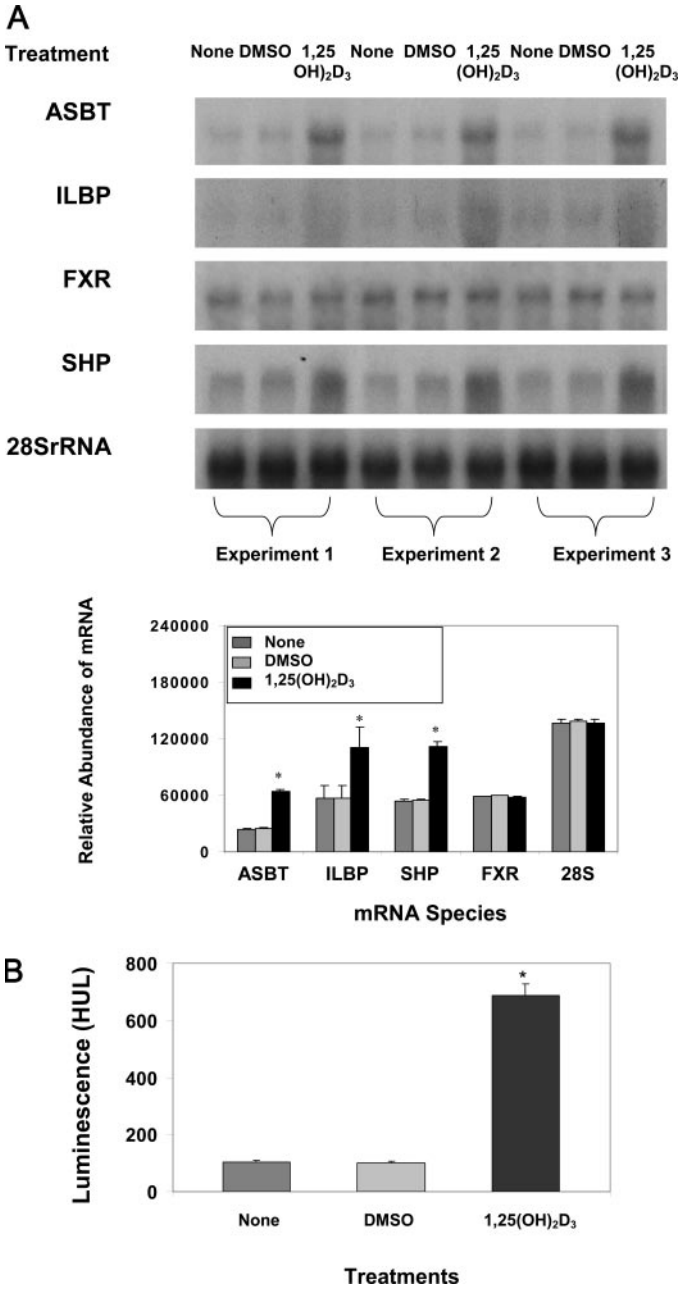

Fig. 9. Human ASBT mRNA expression is induced by of $1,25(OH)_2D_3$. A, Northern blot analysis of mRNA isolated from control or $1,25(OH)_2D_3$-treated Caco-2 cells. The mRNA expression for human ASBT, ILBP, FXR, and SHP was examined by Northern blot analysis of 10 μg of total RNA and quantified using a PhosphorImager. B, analysis of human ASBT promoter construct in transiently transfected Caco-2 cells with SV40 promoter (None), and treated with DMSO or $1,25(OH)_2D_3$. Activity of the human ASBT promoter construct (encompassing the putative VDRE; see Table 2) was induced 4-fold by $1,25(OH)_2D_3$ treatment. The data represent the mean ± S.D. of three preparations. *, $P < 0.05$ compared with controls.

Acknowledgments

We are grateful to Christopher J. Lemke (Vanderbilt University, Nashville, TN) for the technical assistance with the real-time PCR.

References

Ananthanarayanan M, Balasubramanian N, Makishima M, Mangelsdorf DJ, and Suchy FJ (2001) Human bile salt export pump promoter is transactivated by the farnesoid X receptor/bile acid receptor. *J Biol Chem* **276:**28857–28865.

Chen F, Ma L, Al Ansari N, and Shneider B (2001) The role of AP-1 in the transcriptional regulation of the rat apical sodium-dependent bile acid transporter. *J Biol Chem* **276:**38703–38714.

Chen F, Ma L, Dawson PA, Sinal CJ, Schayck E, Gonzalez FJ, Breslow J, Ananthanarayanan M, and Shneider BL (2003) Liver receptor homologue-1 mediates species- and cell line-specific bile acid-dependent negative feedback regulation of the apical sodium-dependent bile acid transporter. *J Biol Chem* **278:**19909–19916.

Chen F, Ma L, Sartor RB, Li F, Xiong H, Sun A-Q, and Shneider B (2002) Inflammatory-mediated repression of the rat ileal sodium-dependent bile acid transporter by c-fos nuclear translocation. *Gastroenterology* **123:**2005–2016.

Chen KS and DeLuca HF (1995) Cloning of the human 1 alpha, 25-dihydroxyvitamin D_3 24-hydroxylase gene promoter and identification of two vitamin D-responsive elements. *Biochim Biophys Acta* **1263:**1–9.

Chomczynski P and Sacchi N (1987) Single-step method of RNA isolation by acid guanidinium thiocyanate-phenol-chloroform extraction. *Anal Biochem* **162:**156–159.

Cong D, Fong AK, Lee R, and Pang KS (2001) Absorption of benzoic acid in segmental regions of the vascularly perfused rat small intestine preparation. *Drug Metab Dispos* **29:**1539–1547.

Crossman MW, Hauft SM, and Gordon JI (1994) The mouse ileal lipid-binding protein gene: a model for studying axial patterning during gut morphogenesis. *J Cell Biol* **126:**1547–1564.

Dawson PA, Hubbert M, Haywood J, Carddock AL, Zerangue N, Christian WV, and Ballatori N (2005) The heteromeric organic solute transporter α-β, Ost_α-Ost_β, is an ileal basolateral bile acid transporter. *J Biol Chem* **280:**6960–6968.

Dawson PA and Markovich D (2002) Regulation of the mouse Nas1 promoter by vitamin D and thyroid hormone. *Pflueg Arch Eur J Physiol* **444:**353–359.

Denson LA, Sturm E, Echevarria W, Zimmerman TL, Makishima M, Mangelsdorf DJ, and Karpen SJ (2001) The orphan nuclear receptor, shp, mediates bile acid-induced inhibition of the rat bile acid transporter, ntcp. *Gastroenterology* **121:**140–147.

Echchgadda I, Song CS, Roy AK, and Chatterjee B (2004) Dehydroepiandrosterone sulfotransferase is a target for transcriptional induction by the vitamin D receptor. *Mol Pharmacol* **65:**720–729.

Goodwin B, Jones SA, Price RR, Watson MA, McKee DD, Moore LB, Galardi C, Wilson JG, Grober J, Zaghini I, et al. (1999) Identification of a bile acid-responsive element in the human ileal bile acid-binding protein gene. Involvement of the farnesoid X receptor/9-cis-retinoic acid receptor heterodimer. *J Biol Chem* **24:**29749–29754.

Hulzebos CV, Wolters H, Plosch T, Kramer W, Stengelin S, Stellaard F, Sauer PJ, Verkade HJ, and Kuipers F (2003) Cyclosporin A and enterohepatic circulation of bile salts in rats: decreased cholate synthesis but increased intestinal reabsorption. *J Pharmacol Exp Ther* **304:**356–363.

Jung D, Fantin AC, Scheurer U, Fried M, and Kullak-Ublick GA (2004) Human ileal bile acid transporter gene ASBT (SLC10A2) is transactivated by the glucocorticoid receptor. *Gut* **53:**78–84.

Jung D, Fried M, and Kullak-Ublick GA (2002) Human apical sodium-dependent bile salt transporter gene (SLC10A2) is regulated by the peroxisome proliferator-activated receptor α. *J Biol Chem* **277:**30559–30568.

Kerner SA, Scott RA, and Pike JW (1989) Sequence elements in the human osteocalcin gene confer basal activation and inducible response to hormonal vitamin D_3. *Proc Natl Acad Sci USA* **86:**4455–4459.

Kramer W, Corsiero D, Friedrich M, Girig F, Stengelin S, and Weyland C (1998) Intestinal absorption of bile acids: paradoxical behaviour of the 14 kDa ileal lipid-binding protein in differential photoaffinity labelling. *Biochem J* **333:**335–341.

Lewis MC, Brieaddy LE, and Root C (1995) Effects of 2164U90 on ileal bile acid absorption and serum cholesterol in rats and mice. *J Lipid Res* **36:**1098–1105.

Lowry OH, Rosebrough NJ, Farr AL, and Randall JR (1951) Protein measurement with the Folin phenol reagent. *J Biol Chem* **193:**265–275.

Macdonald PN, Whitfield GK, Haussler CA, Hocker AM, Haussler MR, and Komm BS (1992) Evaluation of a putative vitamin D response element in the avian calcium binding protein gene. *DNA Cell Biol* **11:**377–383.

Makishima M, Lu TT, Xie W, Whitfield GK, Domoto H, Evans RM, Haussler MR, and Mangelsdorf DJ (2002) Vitamin D receptor as an intestinal bile acid sensor. *Science (Wash DC)* **296:**1313–1316.

Mangelsdorf D, Thummel C, Beato M, Herrlich P, Schutz G, Umesono K, Blumberg B, Kastner P, Mark M, Chambon P, et al. (1995) The nuclear receptor superfamily: the second decade. *Cell* **83:**835–839.

McCarthy TC, Li X, and Sinal CJ (2005) Vitamin D-receptor-dependent regulation of colon multidrug resistance-associated protein 3 gene expression by bile acids. *J Biol Chem* **280:**23232–23242.
Morrison N and Eisman J (1993) Role of the negative glucocorticoid regulatory element in glucocorticoid repression of the human osteocalcin promoter. *J Bone Miner Res* **8:**969–975.
Neimark E, Chen F, Li X, and Shneider BL (2004) Bile acid-induced negative feedback regulation of the human ileal bile acid transporter. *Hepatology* **40:**149–156.
Ozono K, Liao J, Kerner SA, Scott RA, and Pike JW (1990) The vitamin D-responsive element in the human osteocalcin gene. Association with a nuclear proto-oncogene enhancer. *J Biol Chem* **265:**21881–21888.
Rossi SS, Converse JL, and Hofmann AF (1987) High pressure liquid chromatographic analysis of conjugated bile acids in human bile: simultaneous resolution of sulphated and unsulfated lithocholyl amidates and the common conjugated bile acids. *J Lipid Res* **28:**589–595.
Schmassmann A, Angellotti MA, Ton-Nu HT, Schteingart CD, Marcus SN, Rossi SS, and Hofmann AF (1990) Transport, metabolism and effect of chronic feeding of cholylsarcosine, a conjugated bile acid resistant to deconjugation and dehydroxylation. *Gastroenterology* **98:**163–174.
Shneider BL, Dawson PA, Christie D-M, Hardkar W, Wong MH, and Suchy FJ (1995) Cloning and molecular characterization of the ontogeny of a rat ileal sodium-dependent bile acid transporter. *J Clin Investig* **95:**745–754.
Sorscher S, Lillienau J, Meinkoth JL, Steinback JH, Schtiengart CD, Feramisco J, and Hofmann AF (1992) Conjugated bile acid uptate by *Xenopus laevis* oocytes induced by microinjection with ileal poly A+ mRNA. *Biochem Biophys Res Commun* **186:**1455–1462.
Strom M, Sandgren MP, Brown TA, and DeLuca HF (1989) 1,25-Dihydroxyvitamin D_3 up-regulates the 1,25-dihydroxyvitamin D_3 receptor in vivo. *Proc Natl Acad Sci USA* **86:**9770–9773.
Su T and Waxman DJ (2004) Impact of dimethyl sulfoxide on expression of nuclear receptors and drug-inducible cytochromes P450 in primary rat hepatocytes. *Arch Biochem Biophys* **424:**226–234.
Taketani Y, Segawa H, Chikamori M, Morita K, Tanaka K, Kido S, Yamamoto H, Iemori Y, Tatsumi S, Tsugawa N, et al. (1998) Regulation of type II renal Na^+-dependent inorganic phosphate transporters by 1,25-dihyxroxyvitamin D_3. *J Biol Chem* **273:**14575–14581.
Thierry-Palmer M, Tewolde TK, Forte C, Wang M, Bayorh MA, and Emmett NL (2002) Plasma 24,25-dihydroxyvitamin D concentration of Dahl salt-sensitive rats decreases during high salt intake. *J Steroid Biochem Mol Biol* **80:**315–321.
Thummel KE, Brimer C, Yasuda K, Thottassery J, Senn T, Lin Y, Ishizuka H, Kharasch E, Schuetz J, and Schuetz E (2001) Transcriptional control of intestinal cytochrome P-4503A by 1α,25-dihydroxy vitamin D_3. *Mol Pharmacol* **60:**1399–1406.
Traber PG, Gumucio DL, and Wang W (1991) Isolation of intestinal epithelial cells for the study of differential gene expression along the crypt-villus axis. *Am J Physiol* **260:**G895–G903.
Xu G, Shneider BL, Shefer S, Nguyen LB, Batta AK, Tint GS, Arrese M, Thevananther S, Ma L, Stengelin S, et al. (2000) Ileal bile acid transport regulates bile acid pool, synthesis and plasma cholesterol levels differently in cholesterol-fed rats and rabbits. *J Lipid Res* **41:**298–304.
Zierold C, Darwish HM, and DeLuca HF (1994) Identification of a vitamin D-response element in the rat calcidiol (25-hydroxyvitamin D_3) 24-hydroxylase gene. *Proc Natl Acad Sci USA* **91:**900–902.
Zierold C, Darwish HM, and DeLuca HF (1995) Two vitamin D response elements function in the rat 1,25-dihydroxyvitamin D 24-hydroxylase promoter. *J Biol Chem* **270:**1675–1678.

Address correspondence to: Dr. K. Sandy Pang, Faculty of Pharmacy, University of Toronto, 19 Russell St., Toronto, ON M5S 2S2, Canada. E-mail: ks.pang@utoronto.ca